

## Experimental Data Reconstruction Using CFD Results Based on Proper Orthogonal Decomposition

Kanako Yasue  
Shigeru Kuchi-Ishi  
Shigeya Watanabe

Japan Aerospace Exploration Agency  
Tokyo 182-8579  
Japan  
yasue@chofu.jaxa.jp

### Abstract

An experimental fluid dynamics (EFD)/computational fluid dynamics (CFD) integration technique using proper orthogonal decomposition (POD) is developed for reconstructing a flow field of measurement data with equal information as CFD analysis. First, POD modes are extracted from several CFD data sets (snapshots) using a snapshot POD method. Then the entire flow field of measured data can be reconstructed using a “gappy” POD method. In this study, the entire flow field over a DLR-F6 FX2B wind tunnel model is reconstructed from only the measured pressure coefficient ( $C_p$ ) data of pressure ports. Use of pressure-sensitive paint (PSP) data is also examined, and the accuracy of reconstructed results is examined. We show that a flow field can be reconstructed from pressure port data or from PSP data with satisfactory accuracy.

Keywords: EFD/CFD integration method, proper orthogonal decomposition.

### Introduction

In developing aerospace vehicles, wind tunnel tests and computational fluid dynamics (CFD) are widely used for predicting aerodynamic characteristics under actual flight conditions. Both tools, however, have some discrepancy with flight conditions. For example, setting free-stream conditions to mimic flight conditions is usually difficult in wind tunnel tests. The existence of wind tunnel walls and support systems is peculiar to wind tunnel tests. Also, CFD modeling cannot exactly simulate real flight. While many researchers have been working to improve both techniques, it is necessary to combine the advantages of wind tunnel tests and CFD to achieve more highly accurate predictions of aerodynamic characteristics.

In wind tunnel tests and experimental fluid dynamics (EFD), recent measurement techniques ensure that data have high reliability. Moreover, pressure sensitive paint (PSP) and particle image velocimetry (PIV) have made possible the acquisition of surface and spatial data, in addition to point data. However, obtainable variables and regions are still restricted, and data are sometimes partially lost due to instrumental or settings issues. It is therefore difficult to get a complete view of a flow field, even when data sets are measured with a high degree of accuracy. Since CFD can contain a wide variety of physical quantities, it is useful for understanding flow fields in detail. CFD has uncertainty in computational models, however, especially for complicated flow-fields like turbulent flows. Accordingly, CFD results must be validated. The ability to obtain precise measured data with an equivalent amount of information as CFD by applying some kind of integration of EFD and CFD would lead to highly accurate predictions of aerodynamic characteristics. We believe that proper orthogonal decomposition (POD) [1] can play a role in realizing this.

POD extracts dominant components (or modes) from large-scale data sets. It is also known as principle component analysis in the statistical literature [1], or as a Karhunen-Loève expansion in pattern recognition [2, 3], and is widely used in various fields. In fluid dynamics, POD is employed in many applications, such as the extraction of coherent structure in turbulence [4], aeroacoustics [5, 6], fluid control [7, 8], data assimilation [9], and aerodynamic design optimization [10]. The snapshot POD method introduced by Sirovich [4] is usually applied, especially for large-scale problems. In this POD process, data can be represented as a linear combination of POD modes (bases) and expansion coefficients. A set of instantaneous flow solutions (“snapshots”) is used to compute a set of POD modes. POD is also applied to the reconstruction of the incomplete (“gappy”) data set. In that case, a gappy POD method, developed by Everson and Sirovich, is usually employed for reconstructing marred images [11]. In this technique, an incomplete data set can be reconstructed by solving a small linear system, once a set of POD modes is given.

In this research, we aim to reconstruct a flow field that has the same information level as the CFD from limited measurement data by applying an EFD/CFD integration technique based on the snapshot POD and the gappy POD. The POD modes are first extracted from several snapshots of CFD solutions using the snapshot POD method. Then the entire flow field of measured data can be reconstructed for various variables by obtaining the expansion coefficients using the POD modes, and limited experimental data sets can be reconstructed by applying the gappy POD method. In this paper, the reconstruction process using the POD approach is first outlined, and then, several test cases for reconstructing the flow field from measured pressure port data or PSP data are shown.

## Data Reconstruction Method Using Proper Orthogonal Decomposition

The flow field data can be orthogonally decomposed using the POD as a linear combination of POD modes and expansion coefficients, and written as follows:

$$\mathbf{q}_i = \sum_{i=1}^m a_i \phi_i \quad (1)$$

where  $\phi_i$  and  $a_i$  represent a POD mode and an expansion coefficient, respectively. Therefore, the flow field of a measured data set can be reconstructed if the POD modes and the expansion coefficients are determined.

In this POD approach, the POD modes are extracted from a number of CFD solutions that are pre-computed in several free-stream conditions. Given  $m$  snapshots, a set of snapshots is written in matrix form as

$$\mathbf{Q} = \begin{bmatrix} \mathbf{q}_1 & \mathbf{q}_2 & \cdots & \mathbf{q}_m \end{bmatrix} \quad (2)$$

$\mathbf{q}_i$  is the CFD solution vector:

$$\mathbf{q} = \left( \rho_i(1) \cdots \rho_i(n) \quad u_i(1) \cdots u_i(n) \quad v_i(1) \cdots v_i(n) \quad w_i(1) \cdots w_i(n) \quad p_i(1) \cdots p_i(n) \right)^T, \quad (3)$$

where  $\rho$  is the fluid density;  $u$ ,  $v$ , and  $w$  are the Cartesian velocity components;  $p$  is the pressure; and  $n$  is the number of cells or nodes. It is well known that the POD modes can be computed by solving the eigenvalue problem

$$\mathbf{R} \phi_i = \lambda_i \phi_i \quad (i = 1, 2, \cdots, m), \quad (4)$$

where  $\mathbf{R}$  denotes the covariance matrix, written as

$$\mathbf{R} = \mathbf{Q} \mathbf{Q}^T, \quad (5)$$

and  $\lambda$  is the eigenvalue. Note that  $\lambda$  represents the energy contributions of the corresponding POD modes, and is defined as

$$\lambda_1 > \lambda_2 > \cdots > \lambda_m > 0. \quad (6)$$

However the size of the covariance matrix  $\mathbf{R}$  is  $5n \times 5n$  in this case, so its computational costs would be huge. In the snapshot POD method, therefore, the POD modes are constructed by solving a small eigenvalue problem for covariance matrix  $\mathbf{R}'$ :

$$\mathbf{R}' \psi_i = \lambda_i \psi_i \quad (i = 1, 2, \cdots, m). \quad (7)$$

The small covariance matrix  $\mathbf{R}'$  is written as

$$\mathbf{R}' = \mathbf{Q}^T \mathbf{Q}, \quad (8)$$

where  $\psi_i$  is the eigenvalue of matrix  $\mathbf{R}'$ . The size of this matrix  $\mathbf{R}'$  is  $m \times m$ , and  $m$  is usually small compared with the number of cells or nodes of a CFD solution. Finally, the POD modes can be obtained using  $\psi_i$  as in the following equation:

$$\phi_i = \frac{\mathbf{Q}\psi_i}{\sqrt{\lambda_i}} \quad (9)$$

In this study, all POD modes are used because the number of snapshots is very small. However, it is not necessary to use all POD modes to reconstruct the data.

Once the POD modes are determined, the expansion coefficients can be computed from the limited experimental data sets by using the gappy POD method. Let  $g$  be the reconstructed vector that we want to obtain, and consider that the measured data is a part of  $g$  with the following mask vector,

$$m = \begin{cases} 1 & \text{if existing exp. data} \\ 0 & \text{if not existing exp. data} \end{cases} \quad (10)$$

Then the measured data can be also decomposed using the POD approach as

$$\tilde{g}_i = \sum_{i=1}^m b_i \tilde{\phi}_i \quad (11)$$

where  $\tilde{g}$  denotes the measured data set,  $\tilde{\phi}_i$  the POD mode corresponding to  $\tilde{g}$ ,  $b_i$  the expansion coefficient, and  $\tilde{n}$  the number of measurement data. Here the measured data  $\tilde{g}$  and the POD mode  $\phi_i$  are already known, so we can determine the expansion coefficient by applying the least-squares method to minimize the evaluation function  $J$  as,

$$J = \left\| \sum_{i=1}^m b_i \tilde{\phi}_i - \tilde{g} \right\| \rightarrow \min \quad (12)$$

This leads to a simple linear system as follows:

$$\tilde{\Phi}^T \tilde{\Phi} \mathbf{B} = \tilde{\Phi}^T \tilde{g}, \quad (13)$$

where

$$\tilde{\Phi} = \begin{bmatrix} \tilde{\phi}_1 & \cdots & \tilde{\phi}_m \end{bmatrix}, \quad (14)$$

and

$$\mathbf{B} = \begin{bmatrix} b_1 & \cdots & b_m \end{bmatrix}^T. \quad (15)$$

Finally, the flow field for the measured data set can be reconstructed by the following equation:

$$g_i = \sum_{i=1}^m b_i \phi_i \quad (16)$$

## Results and Discussion

### Data reconstruction from measured pressure port data over DLR-F6 FX2B wind tunnel model

We first attempt this approach to reconstruct an entire flow field over a DLR-F6 FX2B model [12, 13] from measured pressure coefficient ( $C_p$ ) data of pressure ports and several CFD results. The experimental data were measured at the JAXA 2 m  $\times$  2 m transonic wind tunnel facility. There are 137 pressure ports located at a total of five cross-sectional surfaces of the left wing (Fig 1). Table 1 shows the free-stream conditions of the experimental data. The Mach number of this measurement data is set to be 0.75, the Reynolds number is 1.5 million, and the angle of attack is 1.5 deg. In this case, seven snapshots, which are the Reynolds-averaged Navier-Stokes solutions computed by a CFD solver FaSTAR [14] together with an automatic unstructured mesh generator HexaGrid [15], are prepared for extracting POD modes. Table 1 also lists free-stream conditions for the snapshots. Note that the free-stream conditions of the experimental data are not included in the CFD results. Total number of cells for each snapshot is about 15 million.

Figure 2 shows the obtained three-dimensional pressure distributions. Using this POD approach, a three-dimensional flow field that is consistent with the experimental data and has same amount of information as a CFD solution can be obtained from limited experimental data sets. The CPU time required to obtain this flow

field was about 2 min using the JAXA supercomputer system (JSS). Since it takes more than 10 h for CFD computation using 40 JSS processing elements, it is advantageous that this POD approach provides the same amount of information as CFD in a much shorter time. Figure 3 shows the  $C_p$  profiles at  $\eta = 0.150, 0.331, 0.514, 0.638,$  and  $0.847$  with those obtained from CFD analysis under the experimental conditions for comparison. As can be seen, the results of this POD approach show much better agreement with the experimental data than do the CFD results.

To confirm that the reconstructed flow field can follow experimental trends other than pressure port sections, the obtained surface  $C_p$  distributions are compared with those obtained by PSP [15], which were measured under the same conditions as the pressure port data. Figures 4 and 5 respectively show the  $C_p$  contours on the upper surface and the  $C_p$  profiles at several spanwise locations. As can be seen, the shock positions of the results obtained by POD are closer to the experimental data than those obtained by CFD computation. This indicates that one can obtain the entire flow field close to the experiment from a limited amount of pressure port data and CFD solutions using this POD approach. As shown in Fig. 5(c), the  $C_p$  profiles located from  $x/c = 0$  to  $x/c = 0.2$  are not improved compared with CFD results. This is because the number of snapshots is insufficient to reconstruct this flow field.

**Table 1: Free-stream conditions for the experimental data and the CFD results (snapshots)**

|                  | Mach number | Reynolds number<br>$\times 10^6$ | Angle of attack<br>[deg] |
|------------------|-------------|----------------------------------|--------------------------|
| Experiment       | 0.75        | 1.5                              | 1.538                    |
| Snapshot 1 (CFD) | 0.75        | 1.5                              | -3.0                     |
| Snapshot 2 (CFD) | 0.75        | 1.5                              | -2.0                     |
| Snapshot 3 (CFD) | 0.75        | 1.5                              | -1.0                     |
| Snapshot 4 (CFD) | 0.75        | 1.5                              | 0.0                      |
| Snapshot 5 (CFD) | 0.75        | 1.5                              | 1.0                      |
| Snapshot 6 (CFD) | 0.75        | 1.5                              | 2.0                      |
| Snapshot 7 (CFD) | 0.75        | 1.5                              | 3.0                      |

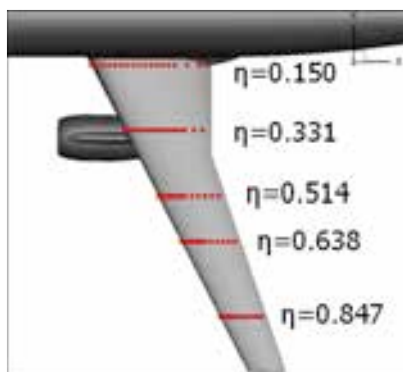


**Fig. 1 Positions of pressure ports.**

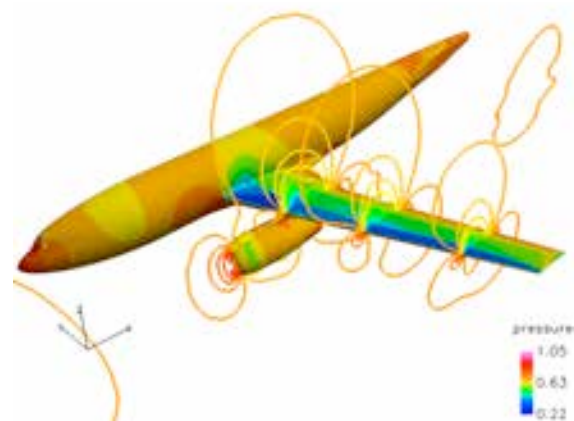


**Fig. 2 Obtained three-dimensional pressure distributions around the DLR-F6 FX2B wind tunnel model.**

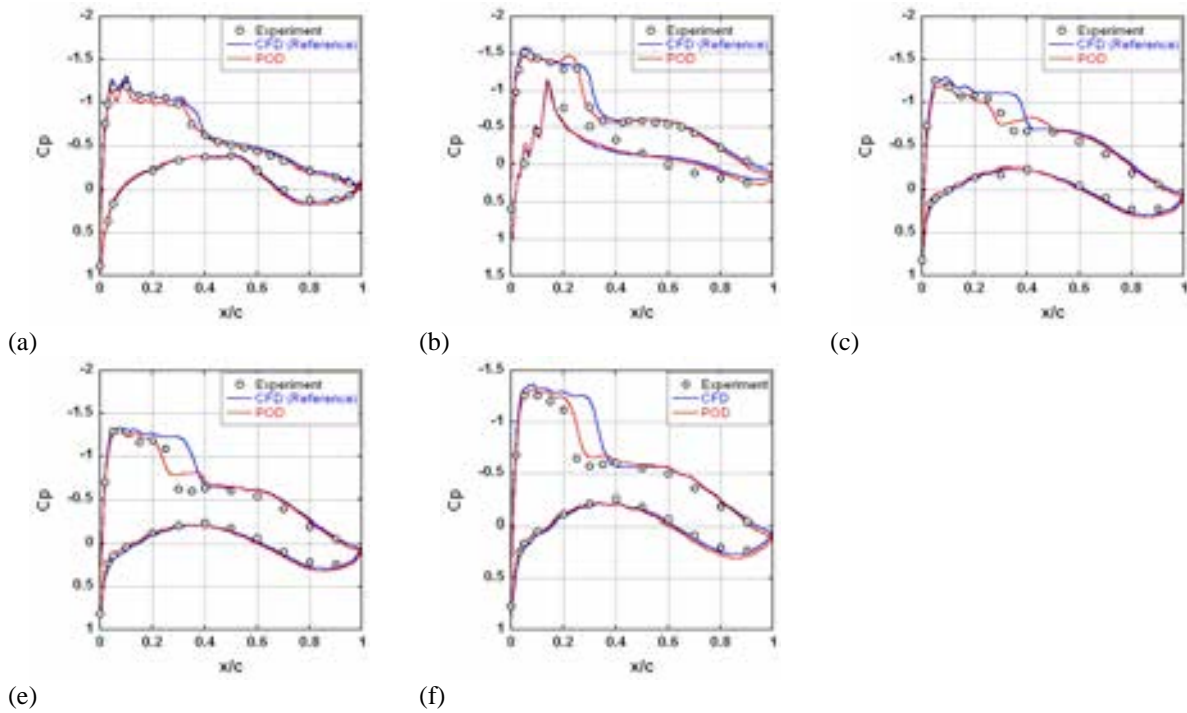


**Fig. 3**  $C_p$  distributions obtained by the POD approach and distributions from experiment and CFD for (a)  $\eta = 0.150$ , (b)  $\eta = 0.331$ , (c)  $\eta = 0.514$ , (d)  $\eta = 0.638$ , and (e)  $\eta = 0.847$ .

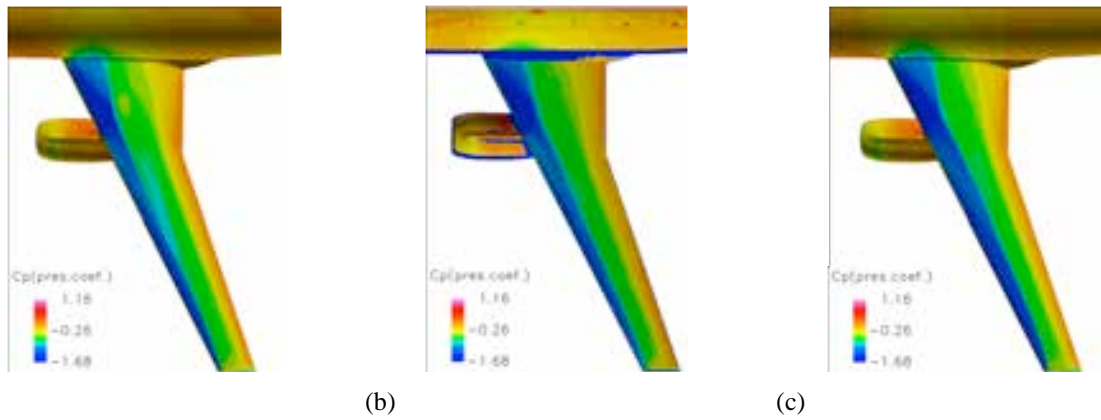


**Fig. 4** Surface pressure distributions obtained by (a) POD approach, (b) PSP measurement (reference data), and (c) CFD (reference data).

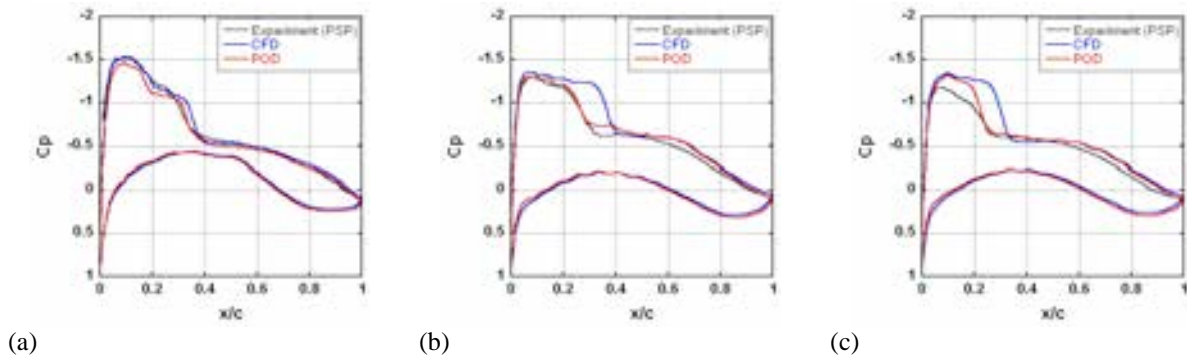


**Fig. 5**  $C_p$  distributions obtained by the POD approach and  $C_p$  distributions from PSP data and CFD for (a)  $\eta = 0.400$ , (b)  $\eta = 0.700$ , and (c)  $\eta = 0.900$ .

## Reconstruction of PSP data measured with the DLR-F6 FX2B wind tunnel model

We next extend this approach to reconstruct an entire flow field from measured PSP data and several CFD results. The PSP data, which has the  $C_p$  distribution over the upper surface shown in Fig. 6, were measured at the JAXA  $2\text{ m} \times 2\text{ m}$  transonic wind tunnel facility [16]. The free-stream conditions of the experimental data are the same as in the previous subsection. The snapshots prepared for this case are also same as in the previous subsection.

The obtained  $C_p$  profiles at several spanwise locations are shown in Fig. 7 with those of the PSP data and the CFD results. We can see that the flow field is successfully obtained from the PSP data. In the PSP measurement, measurement error could occur due to the lighting setup or painting setup as shown near  $x/c = 0$  at the  $\eta = 0.847$  spanwise location in Fig. 7(f). The obtained results using the POD approach, however, provide reasonable profiles without the effect of this measurement error.

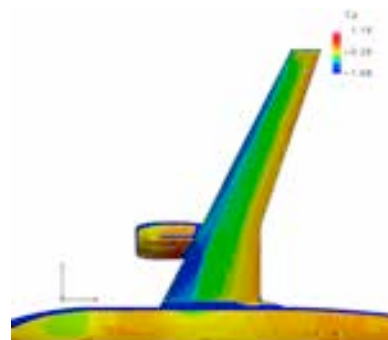


**Fig. 6 The  $C_p$  contours obtained by PSP measurement.**

## Concluding Remarks

An EFD/CFD integration approach utilizing snapshot POD and gappy POD was successfully developed for obtaining the three-dimensional flow field from a limited experimental data set and several CFD solutions. We first attempted this POD approach to reconstruct the flow field over a DLR-F6 FX2B wind tunnel model from its pressure port data and seven CFD solutions. The results showed that the entire flow field can be reconstructed with satisfactory accuracy from a very small amount of measurement data and CFD solutions. Moreover, this POD approach can obtain a flow field that has equal information with the CFD result, in a much shorter time than is required for CFD calculation. In some locations, however, the results farther from the experimental data for the POD approach compared with CFD, because the number of prepared snapshots is insufficient. Thus, the necessary number of snapshots or the snapshot parameters should be examined to improve the results. We next extended this approach to PSP data over the DLR-F6 FX2B model. A reasonable flow field can be obtained, even though measurement error is included in the PSP data.

The results of several test cases indicate that the POD-based EFD/CFD integration approach can be an effective tool for complementing experimental data or predicting entire flow fields, if there are several existing CFD solutions. In future research we will investigate improvements in the accuracy of the present method by a careful understanding and treatment of the obtained POD modes and expansion coefficients.

## Acknowledgements

The authors thank Kazuyuki Nakakita, Kazunori Mitsuo, and Hiroyuki Kato for providing experimental data on the DLR-F6 FX2B wind tunnel model. The authors also thank Atsushi Hashimoto and Keiichi Murakami for providing FaSTAR and HexaGrid, respectively.

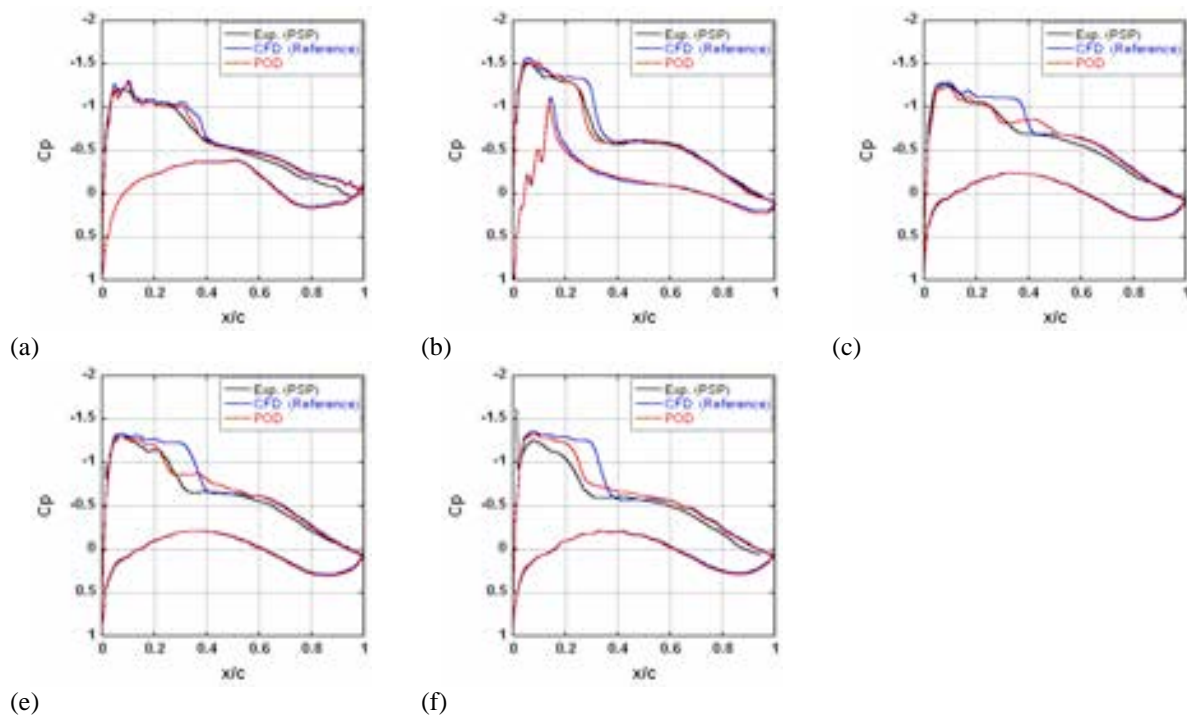


Fig. 7  $C_p$  distributions obtained by the POD approach and distributions from the experimental data and CFD for (a)  $\eta = 0.150$ , (b)  $\eta = 0.331$ , (c)  $\eta = 0.514$ , (d)  $\eta = 0.638$ , and (e)  $\eta = 0.847$ .

## References

- [1] N. Ahmed and M. H. Goldstein, "Orthogonal Transforms for Digital Signal Processing," Springer-Verlag, N. Y., (1975).
- [2] R. B. Ash and M. F. Gardner, "Topics in Stochastic Processes," Academic Press, New York, (1975).
- [3] K. Fukunaga, "Introduction to Statistical Pattern Recognition," Academic Press, New York, (1972).
- [4] L. Sirovich, "Turbulence and the dynamics of coherent structures Part I," *Q. Appl. Math.*, XLV(3) (1987), pp. 561-571.
- [5] C. E. Tinney, L. S. Ukeiley and M. N. Glauser, "Low-dimensional Characteristics of a Transonic Jet. Part 1. Proper Orthogonal Decomposition," *J. Fluid Mech.*, 612(2008), pp.107-141.
- [6] J. B. Freund and T. Colonius, "Turbulence and Sound-field POD Analysis of a Turbulent Jet," *Int'l J. Aeroacoustics*, 8(2009), pp.337-354.
- [7] R. King, "Active Flow Control II," Springer, (2010).
- [8] R. D. Joslin, and D. N. Miller, "Fundamentals and Applications of Modern Flow Control," AIAA Progress in Astronautics and Aeronautics, 231(2009).
- [9] X. Ma, G. E. Karniadakis, H. Park and M. Gharib, "DPIV-driven Flow Simulation: A New Computational Paradigm," *Proc. R. Soc. Lond. A*, 459(2003), pp.547-565.
- [10] T. Bui-Thanh and M. Damodaran, "Aerodynamic Data Reconstruction and Inverse Design Using Proper Orthogonal Decomposition," *AIAA J.*, 42(8) (2004), pp. 1505-1516.
- [11] R. Everson and L. Sirovich, "Karhunen-Loeve Procedure for Gappy Data," *J. Opt. Soc. Am. A*, 12(8) (1995), pp.1657-1664.
- [12] "2nd AIAA Drag Prediction Workshop," <http://aaac.larc.nasa.gov/tsab/cfdlarc/aiaa-dpw/Workshop2/workshop2.html>.
- [13] "3rd AIAA Drag Prediction Workshop," <http://aaac.larc.nasa.gov/tsab/cfdlarc/aiaa-dpw/Workshop3/>.
- [14] A. Hashimoto, K. Murakami and T. Aoyama, "JAXA Digital/Analog Hybrid Wind Tunnel: Development of Digital Wind Tunnel," *JAXA-SP-09-003*, (2010).
- [15] A. Hashimoto, K. Murakami, T. Aoyama and P. Lahur, "Lift and Drag Prediction Using Automatic Hexahedra Grid Generation Method," *AIAA paper 2009-1365*, (2009).
- [16] K. Nakakita, M. Kurita K. Mitsuo and S. Watanabe, "Practical Pressure-Sensitive Paint Measurement System for Industrial Wind Tunnels at JAXA," *Meas. Sci. Tech.*, 17(2005), pp.359-366.